

Cite this article

Nour Eldin M, Naeem A and Kim J (2020)
Seismic retrofit of a structure using self-centring precast concrete frames with enlarged beam ends.
Magazine of Concrete Research 72(22): 1155–1170,
<https://doi.org/10.1680/jmacr.19.00012>

Research Article

Paper 1900012
Received 28/12/2018; Revised 23/05/2019;
Accepted 06/06/2019;
Published online 19/07/2019

Keywords: precast concrete/structural analysis/structural design

ICE Publishing: All rights reserved

Seismic retrofit of a structure using self-centring precast concrete frames with enlarged beam ends

Mohamed Nour Eldin

Assistant Professor, Department of Civil and Architectural Engineering, Sungkyunkwan University, Suwon, Korea

Asad Naeem

Assistant Professor, Department of Civil Engineering, Balochistan University of Information Technology, Engineering and Management Sciences, Quetta City, Pakistan

Jinkoo Kim

Professor, Department of Civil and Architectural Engineering, Sungkyunkwan University, Suwon, Korea
(corresponding author: jkim12@skku.edu)

This research proposes a procedure to retrofit existing structures using self-centring post-tensioned precast concrete (SC-PC) frames. The procedure utilises the initial stiffness of the un-retrofitted structure and predicts the required initial stiffness of the retrofitted one using the N2 method. A modified precast beam-end shape is proposed to double the re-centring moment capacity of the retrofit frame at the beam–column interface. Different retrofit cases for two- and three-dimensional structures utilising the proposed and conventional PC beams are investigated. The results of the proposed procedure are verified through non-linear time history analysis using two different sets of earthquake records compatible with the design-level response spectrum. The study results reveal that the SC-PC retrofit frames are quite effective in controlling the earthquake-induced storey drift of the retrofitted structures while eliminating the residual storey drift. The results also indicate the effectiveness of the proposed beam shape in mitigating the inter-storey drift demand of the analysis model structures.

Notation

A_s	required steel area	m_i	mass assigned to degree of freedom i
a	depth of the equivalent rectangular compression stress block corresponding to the compression force	R	ratio between the acceleration–displacement response spectra slopes of the elastic radial lines of the retrofitted and un-retrofitted structures
b_g	width of grout pad at beam–column interface	S_a	spectral acceleration
D	beam depth without enlargement	S_d	elastic displacement demand
d	beam height	S_{DS}, S_{D1}	spectral acceleration at short period and at 1 s, respectively
E_p	elastic modulus of the prestressing steel	S_0, S_1	slopes of the un-retrofitted structure and retrofitted one on the acceleration–displacement response spectra
F_c	resultant concrete compression force	T	natural period of vibration of the equivalent single-degree-of-freedom system
F_{pt}	force developed in the post-tensioning tendon	t	thickness at the bottom of the enlarged part of the precast beam
f'_c	concrete nominal compressive strength	Γ	modal participation factor
f_{pi}	initial stress in the post-tensioning tendon	ε_{pt}	strain in the post-tensioning tendon
f_{py}	yield strength of the post-tensioning tendon	ρ_{min}	minimum reinforcement ratio
f_u	ultimate steel stress	ρ_t	reinforcement ratio
f_y	steel yield stress	Φ_i	displacement amplitude at degree of freedom i of the fundamental mode shape normalised to have a unit maximum amplitude at the roof
h_g	height of grout pad at interface	$\phi_i, \phi_{(i-1)}$	amplitudes of the normalised mode shape at level i and $i - 1$, respectively
h_i	storey height between storey i and $i - 1$		
I	moment of inertia of beam section based on gross section properties		
K_0	initial stiffness of un-retrofitted structure		
K_{PC}	required stiffness of one self-centring post-tensioned precast concrete (PC) frame		
K_r	required initial stiffness of retrofitted structure		
L	distance between the force developed in the tendon and the resultant compression force developed in the concrete compressive stress block		
M_{cap}	moment capacity of beam–column connection		
M_{decomp}	moment resistance at gap opening of the self-centring post-tensioned PC connections		

Introduction

Two general seismic retrofit approaches are commonly used to increase the strength/stiffness and ductility of structures. The first approach focuses on global modification of the structural

Offprint provided courtesy of www.icevirtuallibrary.com
Author copy for personal use, not for distribution

system, which leads to increasing both the stiffness and the lateral load capacity of the structure. Examples of this approach include the addition of shear walls (Guo *et al.*, 2017; Henry *et al.*, 2016) or bracings (Park *et al.*, 2012) to the existing structures to reduce storey drift and thus decrease ductility demand. The second approach focuses on local modification of certain structural elements for improving the performance of that element to fulfill a specified limit state as the building responds at the design level. Examples of the local retrofit approach include the addition of concrete, steel, or fibre-reinforced polymer composite jackets (Binici and Mosalam, 2007) or by adding passive devices at beam–column connections (Belleri *et al.*, 2017; Kim and Seo, 2003). Between the two approaches, the global modification is more common owing to its effectiveness, relative ease and lower overall cost.

Self-centring retrofitting generally leads to reduced ductility demand, even for the case of partially self-centring systems (Hu and Zhang, 2013). A self-centring scheme using post-tensioned (PT) strands was introduced in many structural systems and proved to be effective in enhancing the seismic performance of the systems. For example, in the case of shear wall systems, Holden *et al.* (2003) tested the seismic performance of precast partially prestressed reinforced-concrete (RC) shear walls that incorporated PT unbonded carbon fibre tendons and steel-fibre-reinforced concrete and found that the system showed decreased lateral drift and damage compared with conventionally reinforced precast concrete (PC) walls. Similar results were observed from the cyclic tests of prestressed PC shear walls (Bedoya-Ruiz *et al.*, 2012). Kurama *et al.* (2006) conducted 11 half-scale experiments to investigate the non-linear reversed cyclic behaviour of a hybrid coupled wall system, in which coupling of concrete walls is achieved by post-tensioning steel beams to the walls using unbonded PT tendons. Hu *et al.* (2012) proposed a new seismic retrofit method for RC frames using self-centring hybrid walls. In this scheme, a special base connection that isolates the wall from its foundation ensures the controlled rocking behaviour of the self-centring hybrid wall. The results revealed that the self-centring shear wall is fairly effective in controlling the seismic response of the retrofitted RC frame while having negligible residual storey drift.

In the case of braced frame systems, Roke (2010) evaluated the seismic performance of self-centring concentrically braced frames (SC-CBFs) with respect to the performance-based design approach and criteria. The results of that study indicated that the system performs well under earthquake loading and that the SC-CBFs are a viable alternative to conventional concentric braced frame (CBF) systems. Eatherton *et al.* (2014) carried out quasi-static cyclic tests of half-scale rocking braced steel frames, which are seismic lateral-force-resisting systems that utilise column-uplifting mechanisms, high-strength PT and replaceable energy-dissipating fuses. The tests demonstrate that the controlled rocking system can satisfy

the performance goals of: (a) maintaining elastic response of the rocking braced frame and post-tensioning up to drift ratios of 2–5%; (b) confining inelastic response to replaceable shear fuses; and (c) achieving near-zero residual drift when the lateral forces are removed. Dezfuli *et al.* (2017) proposed an innovative core-less self-centring (CLSC) brace, which is specified as a retrofit device to be used in conjunction with conventional lateral resisting systems. A parametric study was conducted to find the most cost-effective materials and, at the same time, full self-centring behaviour. Dyanati *et al.* (2017) studied the seismic performance and economic effectiveness of two prototype buildings utilising SC-CBF. These systems were assessed and compared with buildings utilising conventional CBFs by evaluating the annual probabilities of exceeding various damage levels, expected annual losses, life-cycle costs (under seismic hazard) and the economic benefit of using SC-CBFs considering prevailing uncertainties. The results of that study showed that the SC-CBF buildings have lower drift-related losses but higher acceleration-related losses.

Self-centring concrete frames consist of concrete beams and columns horizontally post-tensioned together so that a gap can open at the beam–column interface when subjected to a specific applied moment (Chancellor *et al.*, 2014). The early development of concrete self-centring frames came out of the PC seismic structural systems (PRESSS) project during the 1990s (Priestley, 1991, 1996; Priestley *et al.*, 1999). Self-centring concrete frames have performed well in laboratory seismic testing to limit damage to the structure, and have been implemented in practice (e.g. Buchanan *et al.*, 2011; Englekirk, 2002). Rahman and Sritharan (2007) investigated the seismic performance and performance-based design procedure for a hybrid frame reinforced with a combination of mild steel and unbonded prestressing to establish connections between precast beams and columns. In this research, the seismic performance of two buildings satisfied the performance limits under design-level earthquake input motions. Takeuchi *et al.* (2015) proposed a non-uplifting spine frame system with energy-dissipating members without PT strands; its self-centring function was achieved by envelope elastic-moment frames. The system was applied to an actual building constructed in Japan. Nikbakht *et al.* (2015) investigated analytically the performance of self-centring precast segmental bridge columns with shape memory alloy (SMA) starter bars under non-linear static and lateral seismic loading. The results indicated that, in high-seismicity zones, bridge columns with SMA bars at a higher level of PT forces have a superior performance against earthquake loading. Recently, many researchers have investigated seismic retrofit schemes of structures using self-centring systems (e.g. Cao *et al.*, 2015; Naeem and Kim, 2018; NourEldin *et al.*, 2019; Song and Guo, 2017)

In the current paper, a new and simple retrofit procedure is proposed for selecting the required self-centring PC (SC-PC) frame for seismic retrofit of an existing structure.

Offprint provided courtesy of www.icevirtuallibrary.com
Author copy for personal use, not for distribution

The procedure predicts the required additional stiffness to meet a prescribed limit state criterion and utilises it to select the SC-PC retrofit frame. This means that the proposed procedure utilises a performance-based instead of a force-based procedure for predicting the additional stiffness required for retrofitting. In addition, stiffness graphs are provided to select the appropriate retrofitting frame, which eliminates the trial-and-error time. The procedure eliminates the use of any supplemental energy-dissipating devices because it utilises the elastic response of the structure during the earthquake excitation. Also there is no need to conduct a non-linear time history (NLTH) analysis; instead, the proposed procedure utilises a pushover curve (POC) and demand spectrum only to predict the drift of the structure. This reduces the computational cost

significantly. In the proposed retrofit scheme, a new exterior SC-PC frame is attached with PT unbonded steel strands running parallel to the beams of an existing structure (Figure 1). Moreover, a new beam-end shape that doubles the re-centring capacity at the beam-column interface is introduced, and a parametric study is conducted to validate its effectiveness.

Analytical modelling of the proposed PC frame

In the proposed retrofit scheme, the moment capacity at the beam-column interface is primarily dependent on the depth of the PC beam. Typical PC beams have a rectangular

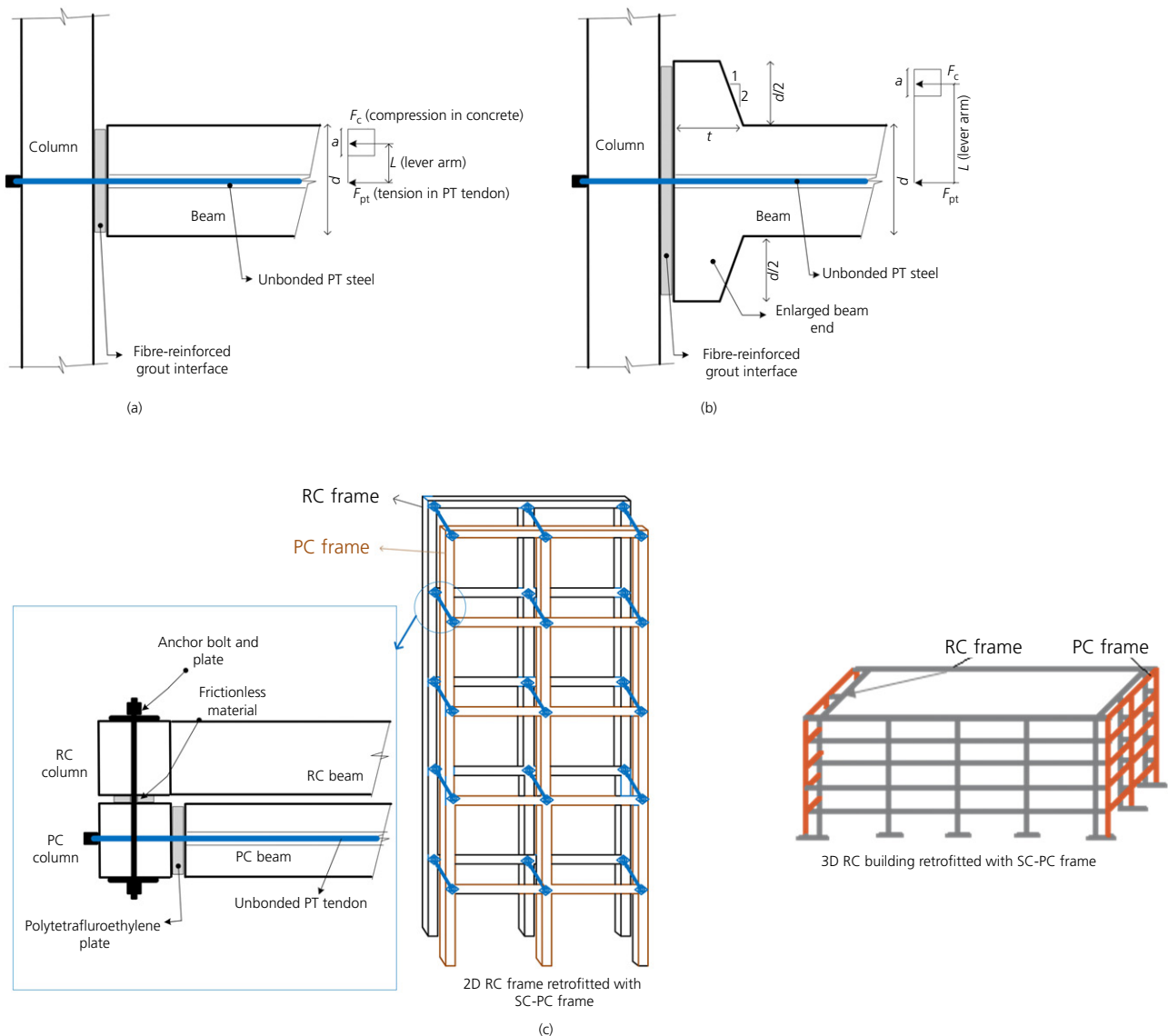


Figure 1. Beam-column interface of the SC-PC retrofit frame: (a) conventional; (b) proposed; (c) implementation of the retrofitting scheme

Offprint provided courtesy of www.icevirtuallibrary.com
Author copy for personal use, not for distribution

cross-section throughout the length. In the current study, the depth of the beam ends is enlarged, as shown in Figure 1. This enlarged part will double the lever arm, which is the distance between the centre of the concrete stress block and the PT tendon. Therefore, if the depth is increased at the beam ends, the moment capacity of the connection and the re-centring force of the system increase proportionally without much increase in the amount of PC concrete. Figure 1(c) shows the retrofit scheme which can be implemented in practice. The existing and the PC columns are connected by a steel anchor rod, and a steel plate is used to tighten the anchor rod and to distribute any additional stress on a larger area at the column face. Commonly, the lateral resisting system lies in the outer perimeter of buildings, and therefore the PC retrofit frames are attached to the outside of the building. The hole diameter in the RC and PC frames is the same as the anchor rod diameter plus some tolerance to allow for a chemical adhesive grout. A frictionless material with proper strength needs to be provided between the existing RC and the retrofit PC frames and around the exposed part of the anchor rod to eliminate any friction between the frames. The anchor rods serve as the main link between the RC and the PC frames to ensure that the PC frame is fully utilised when the RC frame starts to deform laterally. After connecting PC columns to the existing structures, PC beams are placed on seat angles connected to the PC columns, and then the PT steel tendons are placed to connect the PC beams and columns and provide the re-centring capacity.

The stress–strain relation of the PT tendon, which was originally recommended by Mattock (1979) and was used by Celik

and Sritharan (2004) for Grade 270 prestressing strands, is given in Equation 1.

$$1. \quad F_{pt} = \varepsilon_{pt} E_p \left\{ 0.02 + 0.98 \left/ \left[1 + \left(\frac{\varepsilon_{pt} E_p}{1.04 f_{py}} \right)^{8.36} \right]^{1/8.36} \right. \right\}$$

where E_p is the elastic modulus of the prestressing steel; ε_{pt} is the strain in the PT tendon; and f_{py} is the yield strength of the PT tendon.

The moment capacity of the beam–column connection, M_{cap} , is calculated by multiplying the force developed in the PT tendon, F_{pt} , by the distance to the resultant concrete compression force, F_c , as shown in Figure 2. From equilibrium

$$2. \quad F_c = F_{pt}$$

Based on that, the moment capacity of the beam–column connection is obtained as follows

$$3. \quad M_{cap} = F_{pt} (h_g - a)/2$$

where a is the depth of the equivalent rectangular compression stress block corresponding to the compression force, which can be determined using the following equation (ACI, 2014)

$$4. \quad a = F_c / 0.85 f'_c b_g$$

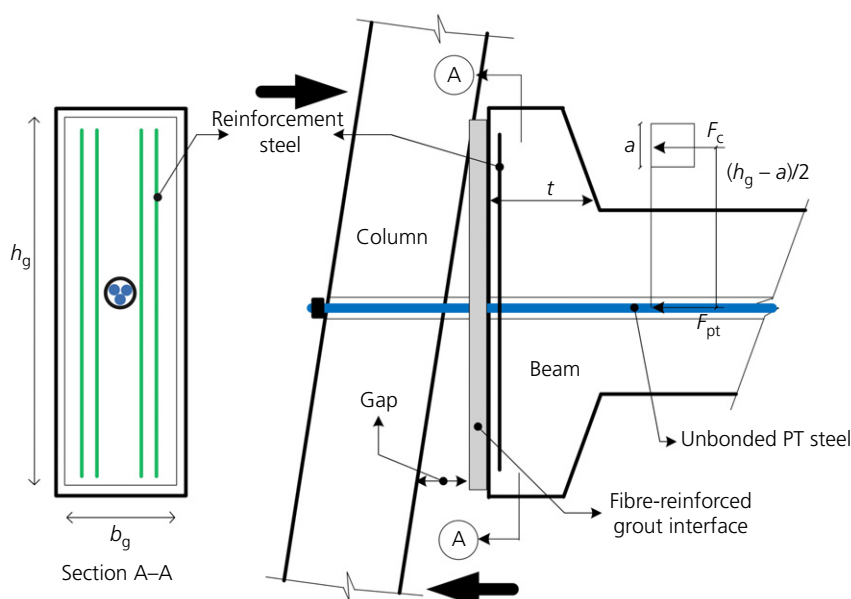


Figure 2. A schematic view of the interface connection between beam and column under an applied moment

where F_c is the concrete compression force; b_g is the width of the grout pad at the beam–column interface; and f'_c is the unconfined concrete compression strength. At yield of the PT tendon, M_{cap} can be calculated as

$$5. \quad M_{cap} = F_{py} (h_g - a)/2$$

The decompression point defines the beginning of a gap opening at the connection interface and corresponds to the condition when the stress in the extreme concrete compression fibre reaches zero at the beam end adjacent to the column. Accounting for the precompression introduced by the initial prestressing force, and assuming a linear strain distribution at the critical section, the following equation is used to determine the moment resistance at gap opening, M_{decomp} (Celik and Sritharan, 2004)

$$6. \quad M_{decomp} = f_{pi} I / \left(\frac{h_g}{2} \right)$$

where f_{pi} is the initial stress in the PT tendon; I is the moment of inertia of the beam section based on the gross section properties; h_g is the height of the grout pad at the interface.

At the beam–column interface, a bilinear elastic spring is used where the gap opening starts between the column and the beam at the decompression level in the PT tendons. When the applied moment exceeds M_{decomp} , the gap increases and the PT tendons start to elongate.

In order to prevent any potential failure at the horizontal face of the enlarged part, reinforcement steel should be provided as shown in section A–A in Figure 2. The minimum moment expected to be resisted by this reinforcement should equal the moment capacity (M_{cap}) of the beam–column connection as calculated above. One may select an approximate value of tension reinforcement ratio ρ equal to or less than ρ_t , but greater than the minimum (ACI-318-14, item 10.5.1 (ACI, 2014)), where the reinforcement ratio ρ_t is given by

$$7. \quad \rho_t = 0.319\beta_1 f'_c / f_y$$

but it should not be less than

$$8. \quad \rho_{min} = 3\sqrt{f'_c} / f_y$$

The required steel area A_s is

$$9. \quad A_s = \rho b t$$

where t is the distance shown in Figure 2 and f_y is the steel yield stress.

Proposed seismic retrofit procedure

In many countries some existing buildings have not been designed based on seismic code provisions. Even buildings designed for seismic loads may experience some non-linearity before reaching the limit state provided by the seismic guidelines. The current research is targeting existing buildings that can experience minimum non-linearity (formation of plastic hinges at beam and column ends) and small residual drift. In the current procedure, the inherent energy-dissipation capacity of the un-retrofitted structure will be utilised (formation of plastic hinges at beam and column ends). The decision to add SC-PC frames for seismic retrofit is made for two main reasons. First, the self-centring capability is needed to eliminate the potential small residual drift in the existing building. Second, the maximum response of the existing building needs to be limited to minimal or no non-linear range.

In this section, a simplified procedure for designing the precast retrofit frame is presented and validated through case studies. In the following sections, the elements of the proposed procedure are discussed in detail. It is worth mentioning that the proposed procedure depends primarily on modifying the elastic stiffness of the existing building using the SC-PC frames based on a prescribed drift limit state (e.g. the maximum inter-storey drift ratio (MIDR) = 1.0%). The additional stiffness added by the SC-PC frames is calculated to achieve this target MIDR using acceleration–displacement response spectra (ADRS) for the combined building and SC-PC frames. The proposed design procedure is as follows.

- (a) Perform pushover analysis for a series of two-dimensional (2D) SC-PC frames with a different number of storeys and bays. Frame dimensions, beam and column cross-sections and the PT tendons' cross-sectional area are chosen to be the most common values used for building structures. Column width should be at least equal to that of the beam to ensure that the concrete compression stress block will be developed across the whole width of the beam.
- (b) Plot the relationship between the initial stiffness, the number of storeys and the bay number for the SC-PC frames only. Three points for each storey are enough to draw a trend line.
- (c) Draw the POC of the un-retrofitted building structure and obtain the initial stiffness of the structure. It is assumed that the response of the structure is dominated by the fundamental vibration mode. Transform the POC of the un-retrofitted structure to a capacity curve on ADRS format. The elastic displacement demand S_d can be directly determined

Offprint provided courtesy of www.icevirtuallibrary.com
Author copy for personal use, not for distribution

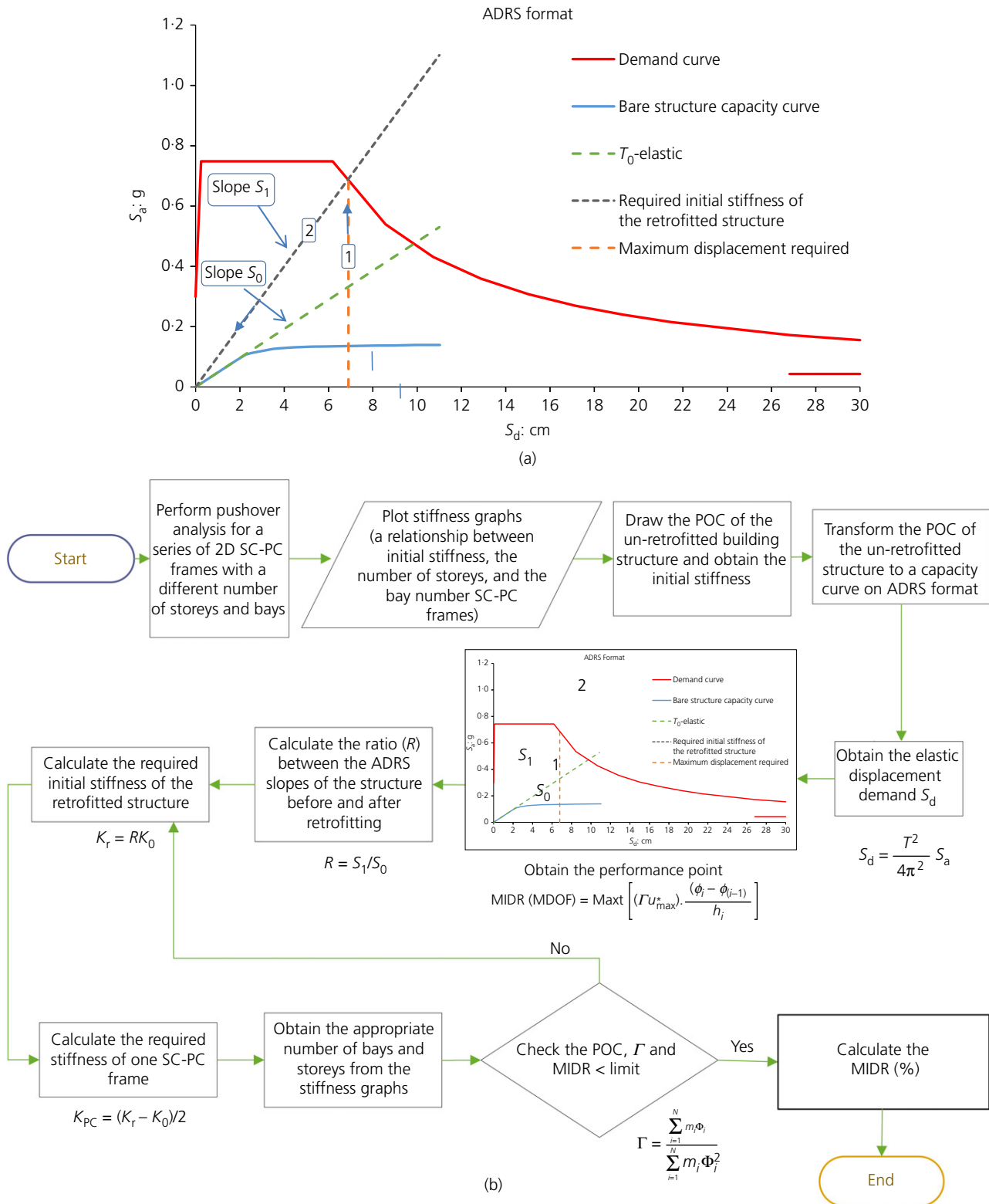


Figure 3. (a) Demand and capacity curves of the bare structure on ADRS format. (b) Flowchart of the proposed procedure

Offprint provided courtesy of www.icevirtuallibrary.com
Author copy for personal use, not for distribution

from the pseudo-acceleration S_a of the response spectrum as

$$10. \quad S_d = \frac{T^2}{4\pi^2} S_a$$

where T is the natural period of vibration of the equivalent single-degree-of-freedom (ESDOF) system. Obtain the performance point using the N2 method (draw a radial line from the origin coinciding with the linear elastic part of the capacity curve) using the equal displacement rule. More details about the N2 method can be found elsewhere (e.g. Fajfar, 2000).

- (d) Calculate the MIDR using the first mode shape of the structure. The MIDR of the structure can be obtained based on the maximum response of the ESDOF system (i.e. the performance point of the ADRS format, which is the intersection between the elastic demand curve and the radial line) as follows

$$11. \quad \text{MIDR(MDOF)} = \text{Max} \left[(\Gamma u_{\text{max}}^*) \frac{(\phi_i - \phi_{(i-1)})}{h_i} \right]$$

where MDOF stands for multiple degree of freedom, u_{max}^* is the maximum displacement of the ESDOF; ϕ_i and $\phi_{(i-1)}$ are the amplitudes of the normalised mode shape at level i and $i-1$, respectively; h_i is the storey height between storeys i and $i-1$; and Γ is the modal participation factor defined as follows

$$12. \quad \Gamma = \frac{\sum_{i=1}^N m_i \Phi_i}{\sum_{i=1}^N m_i \Phi_i^2}$$

where m_i is the mass assigned to DOF i and Φ_i is the displacement amplitude at DOF i of the fundamental mode shape normalised to have a unit maximum amplitude at the roof.

- (e) Draw a vertical line in the ADRS format representing the required MIDR (e.g. at $S_d = 6.9$ cm); see Figure 3(a). Obtain the performance point using the N2 method (the intersection point of the vertical line and the demand curve). Draw a line from the origin to the intersection point of the vertical line with the demand curve. This line coincides with the initial elastic part of the required retrofitted structure. Calculate the ratio (R) between the ADRS slopes of the two radial lines, as show

$$13. \quad R = S_1/S_0$$

where S_0 and S_1 are the slopes of the un-retrofitted structure and retrofitted one on the ADRS format.

- (f) Calculate the required stiffness of the retrofitted structure. Assume that the conversion parameters between the capacity curve on the ADRS format and the POC (the modal participation factor) will be increased by 3% to 5%. This assumption will be verified after constructing the POC of the retrofitted structure.

$$14. \quad K_r = RK_0$$

where K_r is the required initial stiffness of the retrofitted structure; K_0 is the initial stiffness of the un-retrofitted structure; and R is the ratio between the ADRS slopes of the elastic radial lines of the retrofitted and un-retrofitted structures.

- (g) Calculate the required stiffness of one SC-PC frame (one frame on each side of the building is assumed).

$$15. \quad K_{PC} = (K_r - K_0)/2$$

where K_{PC} is the required stiffness of one SC-PC frame.

- (h) Using K_{PC} , obtain the appropriate number of bays and storeys from the stiffness graphs using the trend line

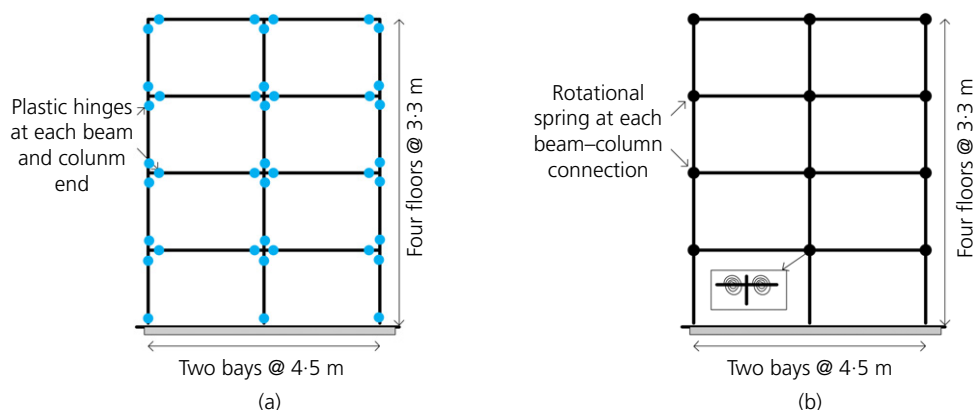


Figure 4. 2D analysis model and the SC-PC frame for retrofit: (a) bare frame; (b) SC-PC frame

Offprint provided courtesy of www.icevirtuallibrary.com
 Author copy for personal use, not for distribution

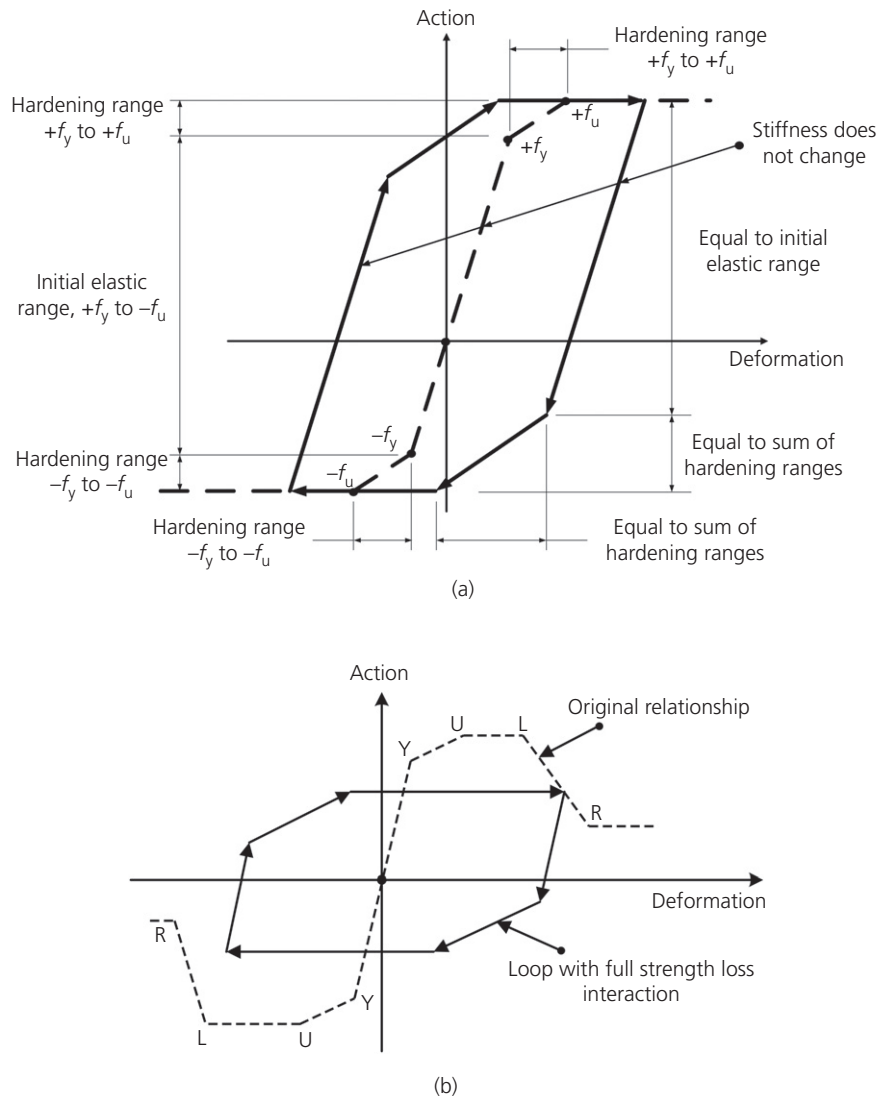


Figure 5. Hysteresis loops of RC (a) columns and (b) beams. L, collapse prevention; R, reduced resistance; U, ultimate strength; Y, yield

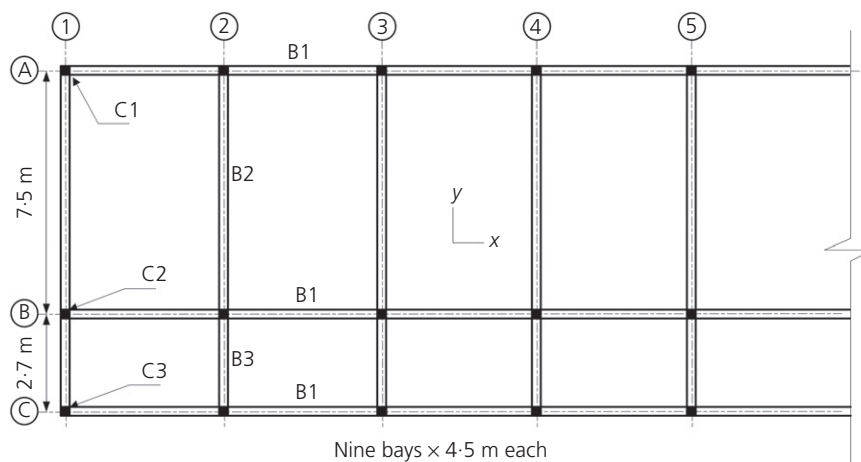


Figure 6. Typical plan of the 3D model structure

Offprint provided courtesy of www.icevirtuallibrary.com
Author copy for personal use, not for distribution

equation on the graph or graphically by drawing a horizontal line at the value of the required stiffness

- (i) Draw the POC of the retrofitted building structure and obtain its initial stiffness from the POC and compare it with the calculated one. In addition, compare the modal participation factor of the retrofitted and un-retrofitted structures. The difference should be within 3 to 10% of the value for a bare structure. This step is for checking only.
- (j) Calculate the maximum inter-storey drift ratio MIDR (%) using the first mode shape of the retrofitted structure. The fundamental mode shape is normalised with respect to the roof displacement.

Figure 3(b) shows a flowchart of the proposed procedure. The N2 method (Fajfar, 2002; Eurocode 8 (CEN, 2004)) combines the pushover analysis of an MDOF model with the response

spectrum analysis of an ESDOF system. The method is based on using inelastic spectra to avoid iterations when evaluating the required demand response quantities. In general, the N2 method is suitable for structures dominated by the first mode. Moreover, in the medium- and long-period ranges, the equal displacement rule generally applies. That is, the displacement of the inelastic SDOF system is equal to the displacement of the corresponding elastic SDOF system with the same period. Smooth, elastic response spectra are used to determine the inelastic response spectra by using reduction factors, which are consistent with elastic response spectra. It is assumed that the distribution of deformations through the structure in the POA approximately corresponds to what is obtained from the dynamic analysis. The expected seismic performance of the building can be assessed by comparing the seismic demands with the capacities for the relevant performance level.

Table 1. Reinforcement details of 3D model structural elements

Designation	Dimensions: mm	Longitudinal reinforcement	Transverse reinforcement
Beam			
B1	550 × 250	D19, 3 top and 3 bottom	D10, 2 legs @ 200 mm
B2	500 × 350	D19, 6 top and 6 bottom	D10, 2 legs @ 200 mm
B3	500 × 350	D19, 4 top and 4 bottom	D10, 2 legs @ 200 mm
Column			
C1	450 × 450	D19, 8	D10, 2 legs @ 200 mm
C2	400 × 425	D19, 8	D10, 2 legs @ 200 mm

Table 2. Variables and parameters required for the proposed procedure for the case studies

Parameter/variable	Value of the parameter/factor		
	2D structure (enlarged beam)	3D structure (enlarged beam)	3D structure (prismatic beam)
K_0	$V/D = 41$ kN/cm	$V/D = 835$ kN/cm	$V/D = 835$ kN/cm
(S_d/D)	$S_d/D = 1/1.26$	$S_d/D = 1/1.16$	$S_d/D = 1/1.16$
(S_a/V) , factors to transform the POC of the bare structure to ADRS format	$S_a/V = 1/1283$ (two bays, four storeys)	$S_a/V = 1/2717$ (nine bays, four storeys)	$S_a/V = 1/2717$ (nine bays, four storeys)
(S_a, S_d) , the performance point of the un-retrofitted structure	(0.38 g, 13.0 cm)	(0.48 g, 9.8 cm)	(0.48 g, 9.8 cm)
$MIDR_{(un-retrofitted)}$	1.6%	1.26%	1.26%
$MIDR_{(required)}$	1.0%	1.0%	1.0%
(S_a, S_d) , the required performance	(0.7 g, 6.8 cm)	(0.65 g, 6.9 cm)	(0.65 g, 6.9 cm)
R	$(0.7 \text{ g} / 6.8 \text{ cm}) / (0.38 \text{ g} / 13.0 \text{ cm}) = 3.5$	$(0.65 \text{ g} / 6.9 \text{ cm}) / (0.45 \text{ g} / 9.8 \text{ cm}) = 1.9$	$(0.65 \text{ g} / 6.9 \text{ cm}) / (0.45 \text{ g} / 9.8 \text{ cm}) = 1.9$
K_r	$= 3.5 \times 41$ kN/cm = 143.5 kN/cm	$= 1.9 \times 835$ kN/cm = 1605 kN/cm	$= 1.9 \times 835$ kN/cm = 1605 kN/cm
K_{PC}	$(143.5 - 41) = 102.5$ kN/cm	$(1605 - 835) / 2 = 385$ kN/cm	$(1605 - 835) / 2 = 385$ kN/cm
Number of bays	2 ($K = 104$ kN/cm)	9 (for frame with nine bays on four storeys, $K = 416$ kN/cm)	9 (for frame with nine bays on four storeys, $K = 351$ kN/cm)
$K_{r(calc)} = (V/D)$	143.2 kN/cm	1675 kN/cm	1560 kN/cm
$K_{retrofitted (calc)} / K_{retrofitted (req)}$	$(143.2 / 143.5) = 0.99$	$(1675 / 1605) = 1.04$	$(1560 / 1605) = 0.97$
$\Gamma(retro) / \Gamma(un-retro)$	$1.24 / 1.26 = 0.98$	$1.2 / 1.13 = 1.06$	$1.22 / 1.13 = 1.08$
$MIDR_{(retrofitted)}$	$MIDR = 0.84\%$	$MIDR = 0.92\%$	$MIDR = 1.0\%$

Offprint provided courtesy of www.icevirtuallibrary.com
Author copy for personal use, not for distribution

Case studies

In this section, two case studies are carried out to verify the proposed design steps explained before. The first case study is a 2D frame model and the second is a three-dimensional (3D)

four-storey school building. In both cases, the modified beam section is utilised in the SC-PC frame. In addition, for comparison purposes, the 3D case is reanalysed using the conventional beam section in the SC-PC retrofit frame and the results

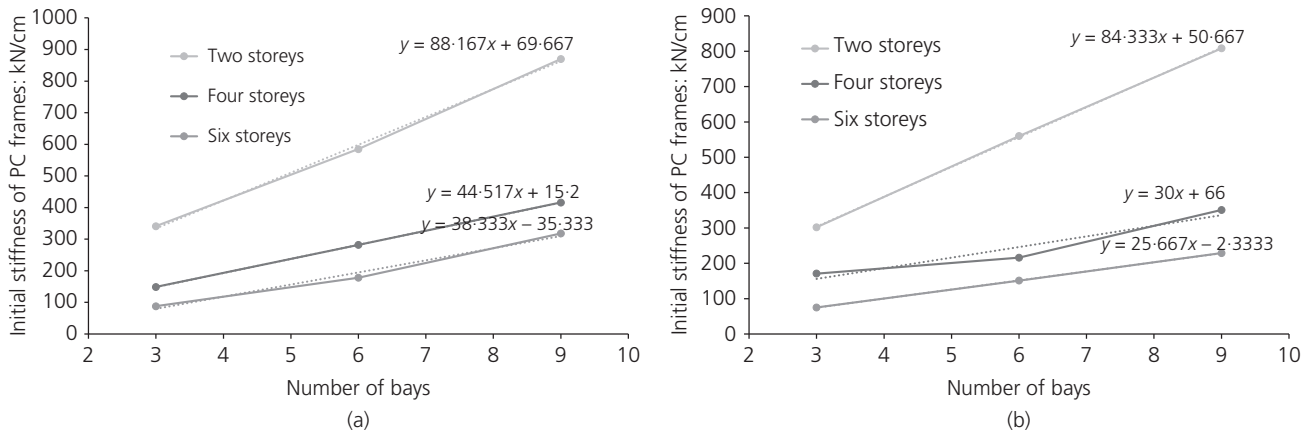


Figure 7. The stiffness graphs of the SC-PC frames: (a) proposed beam section; (b) conventional beam section

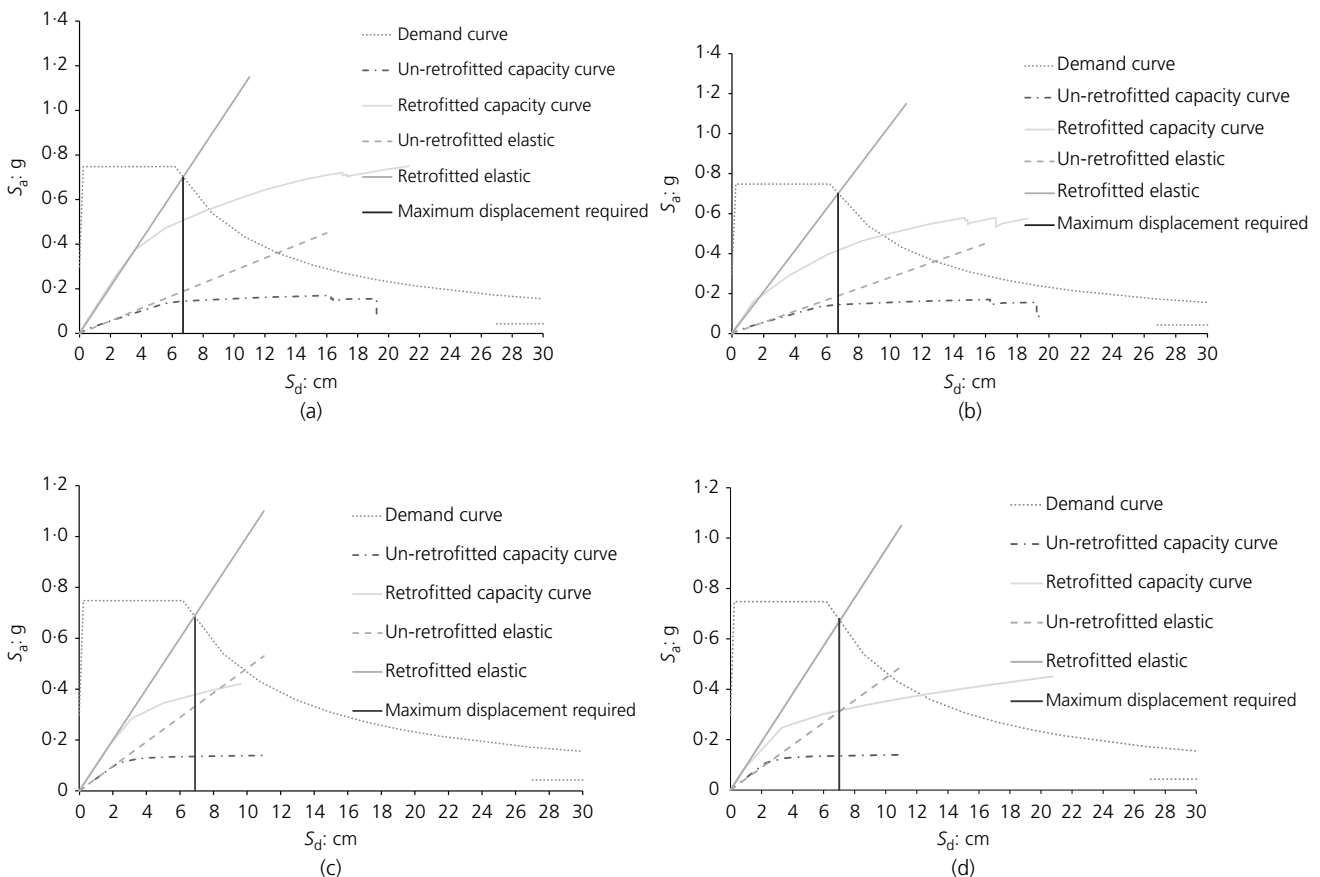


Figure 8. ADRS format of the model structures: (a) 2D frame model using the proposed beam section; (a) 2D frame model using the conventional beam section; (c) 3D structure using the proposed beam section; (d) 3D structure using the conventional beam section

Offprint provided courtesy of www.icevirtuallibrary.com
Author copy for personal use, not for distribution

Table 3. List of the earthquake records used in the time history analysis

Model	Earthquake no.	Earthquake name	PEER code	Station	Scale factor
2D	1	Tabas (Iran)	RSN-138	Boshrooyeh	4.40
	2	Cape Mendocino (CA, USA)	RSN-826	Eureka – Myrtle and West	2.93
	3	Landers (CA, USA)	RSN-862	Indio – Coachella Canal	3.85
3D	1	Landers (CA, USA)	RSN-838	Barstow	2.30
	2	Kocaeli (Turkey)	RSN-1148	Arcelik	2.90
	3	Kocaeli (Turkey)	RSN-1161	Gebze	1.60

are compared with those of the case using the modified beam section to show its effectiveness.

The 2D case study structure

Figure 4 shows the analysis model of the 2D RC bare frame and the SC-PC frame. The four-storey frame has beam sections of 250×500 mm and column sections of 400×450 mm in all storeys. Three longitudinal reinforcement bars (D19) are used at the top and bottom of the beam, and eight longitudinal reinforcement bars (D19) are used for the column. Both beams and columns have D10 @ 200 mm transverse reinforcement. The compressive strength of the concrete is taken as 25 MPa and 280-grade steel is used for the reinforcement bars. The moment frame is designed for gravity loads, resisting a dead load of 7.0 kN/m^2 and a live load of 2.0 kN/m^2 . The sections are assumed to be in a cracked condition and the moments of inertia of the beam and the column sections are reduced to 40% and 70% of the values in a nominal un-cracked condition, respectively. A modal damping of 5% of the critical damping is used in the analyses, and material non-linearity is accounted for by defining localised plastic hinges at the ends of the structural elements. The analysis model for beam elements is composed of two end rotation type moment hinges defined based on ASCE/SEI 41-13 (ASCE, 2013). The hysteresis loops of the beams and columns used in the dynamic analysis of the model structure are shown in Figure 5. The non-linear static analysis required for the proposed procedure is performed using SAP2000 (CSI, 2015) software.

For the SC-PC retrofit frame (Figure 4(b)), the yield strength of the PT tendons, f_{py} , is 1757 MPa and the initial stress after losses, f_{pi} , is 820 MPa; grout strength is taken as 64.0 MPa and the nominal compressive concrete strength, f_c , is 34.0 MPa. Three tendons are used, each with a diameter of 12.7 mm; the width and depth of the beams and columns are 300 and 600 mm, respectively. The retrofit frame is connected with the bare frame at each floor to maintain a rigid diaphragm at each level. Guidelines for such a type of connection are given elsewhere (e.g. Rahman and Sritharan, 2007).

The 3D case study model structure

The SC-PC frame is applied for seismic retrofit of a four-storey RC structure designed only for gravity loads based on the

assumption that it was built when no seismic design code was applied. Figure 6 shows the structural plan of the 3D analysis model structure. The SC-PC frame is aligned along the axes A and C outside the structure, while being rigidly connected to the existing structure at each floor level. The 3D structure has four storeys and the height of each storey is 3.3 m; the sizes of beams and columns are kept constant throughout the height of the structure. Dead and live loads of 4.8 kN/m^2 and 2.5 kN/m^2 , respectively, are used in the structural design. The concrete is assumed to have a nominal compressive strength,

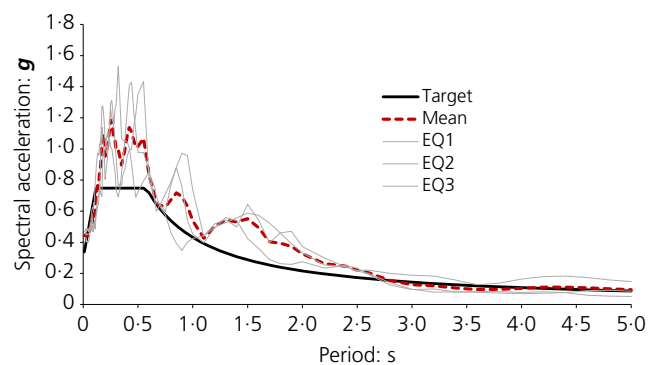


Figure 9. Response spectra of the time history records and target design spectrum (used for 2D model structure)

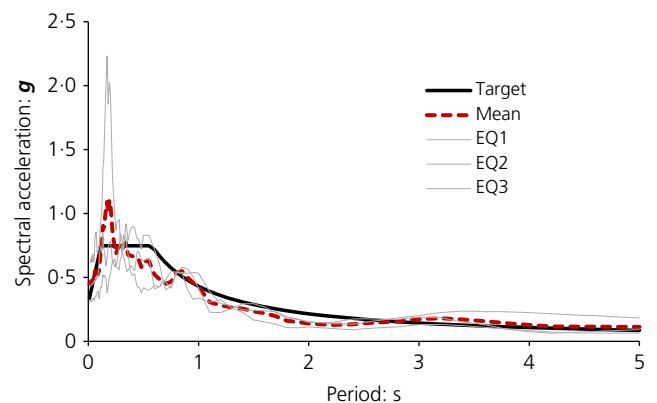


Figure 10. Response spectra of the time history records and target design spectrum (used for 3D model structure)

Offprint provided courtesy of www.icevirtuallibrary.com
Author copy for personal use, not for distribution

f'_c , of 25 MPa and a unit weight of 23.5 kN/m³. The yield stress of reinforcing bars, f_y , is 340 MPa. Beam and column reinforcement details are shown in Table 1. The building is assumed to be located on the site class SD soil with the spectral acceleration coefficients of $S_{DS}=0.70$ and $S_{D1}=0.38$ based on ASCE 7-16 (ASCE, 2016) format.

Results of the case studies

In this section, the results of the 2D and 3D case studies for seismic retrofit using the SC-PC frame are explained. Table 2 summarises the parameters required for the proposed procedure used in each case study. Figure 7 shows the graphs that relate the stiffness, number of storeys and number of bays of the SC-PC frames for two beam section cases: (a) proposed (enlarged) beam sections; (b) conventional (prismatic) beam

sections. The conventional beams have the dimensions of 300 × 600 mm, while the proposed beams have their ends enlarged, as shown in Figure 1. Figure 8 shows the demand and capacity curves of the model structures (2D and 3D case studies) along with the radial elastic lines showing the elastic behaviour of each case on the ADRS format.

Table 2 shows the variables and parameters required for the proposed procedure for three different cases. Two cases are based on the proposed beam-end shapes for the 2D and 3D models, which are indicated in the table as '2D structure (enlarged beam)' and '3D structure (enlarged beam)'. The third case is based on the conventional (prismatic) beam for the 3D model only. Based on the information given in the table, the number of

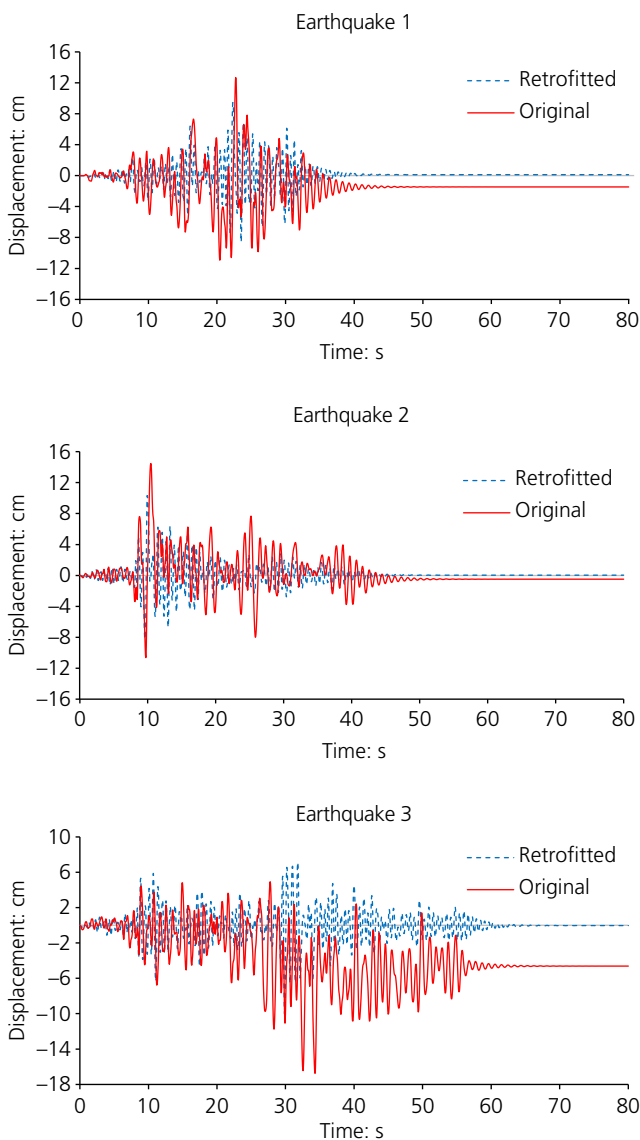


Figure 11. Roof displacement–time history of the 2D model with the proposed beam-end shape of SC-PC frame

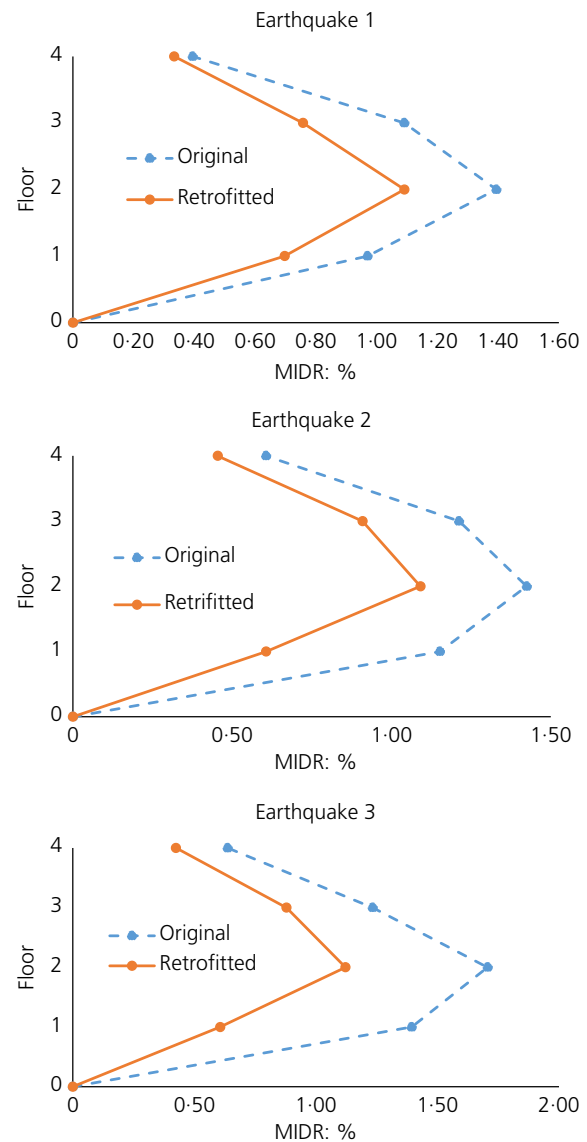


Figure 12. The MIDR of the 2D model structure retrofitted with the SC-PC frame having the proposed beam-end shape subjected to the selected earthquake ground motions

Offprint provided courtesy of www.icevirtuallibrary.com
Author copy for personal use, not for distribution

bays required for the retrofitting of the 3D model is determined to be nine with the characteristics of the SC-PC frame shown in Figure 4(b). It is essential to note that the SC-PC frame characteristics (tendon size, tendon yield strength, beam and column dimensions, etc.) can be easily changed and reflected in the stiffness graphs (i.e. Figure 7). Table 2 shows that the required MIDR has been met for each case: 0.84, 0.92 and 1.0% for the 2D (proposed), 3D (proposed) and 3D (conventional) beams, respectively. For comparison purposes, a different number of bays (e.g. six bays and three bays) of retrofit frames using the proposed beam end are investigated for the 3D model structure, and the MIDR is found to be 1.02 and 1.15% for the six-bay and three-bay structures, respectively.

Verification of the proposed methodology using non-linear dynamic analysis

In this section, the results of the proposed procedure are verified through a comparison with the NLTH analysis results. The seismic performances of the retrofitted and bare structures are evaluated for the 2D and 3D cases using the proposed beam-end shape.

Earthquake records and response spectra

Non-linear dynamic analysis-based seismic performance assessment is carried out using earthquake records obtained from the Pacific Earthquake Engineering Research Centre (PEER) NGA database (PEER, 2017). A different set of ground motion records is used for the 2D and 3D models, as shown in Table 3. Figures 9 and 10 show the design spectra and the scaled response spectra of the earthquake records for the 2D and 3D model structures, respectively. The records are scaled to have a mean spectrum that matches the design response spectrum at the natural period of the structure.

The NLTH analyses of the model structures are performed using SAP2000 (CSI, 2015) software. The beams and columns of the original structure are modelled as member elements with plastic hinges concentrated at both ends. Columns are fixed at the base and all column and beams are rigidly connected. For the SC-PC frame, the beams are modelled as member elements with a multi-linear elastic link at both ends of the beams. Columns are modelled as member elements and are fixed at the base.

Seismic performance evaluation

Figure 11 shows the displacement–time history of the top floor of the 2D model retrofitted with SC-PC frame using the proposed beam-end shape subjected to the selected earthquake ground motions. As can be seen, the retrofit scheme almost eliminates the residual drift when compared to the un-retrofitted case. Figure 12 shows the MIDR of the 2D model structure for the selected earthquake ground motions. The figure reveals that the self-centring scheme is quite effective in controlling the MIDR of the retrofitted frame. Almost one-third of the MIDR is reduced for all cases of earthquake records compared to the un-retrofitted case.

Table 4 summarises the maximum roof displacement, the residual drift and the MIDR of the 2D and 3D models using the proposed procedure and NLTH analysis. The average of the three earthquake records is used for comparison with the proposed method. As can be observed from the table, the retrofit scheme was effective in reducing the maximum roof displacement, the residual drift and the MIDR of the original model. For example, maximum roof displacement is reduced from 145.3 mm to 98.7 mm, the residual drift is reduced from 23.3 mm to zero, and the MIDR is reduced from 1.5% to

Table 4. The response of the 2D and 3D models before and after the retrofit

Model	Number of bays		Maximum displacement: mm	Residual displacement: mm	MIDR: %
2D					
Un-retrofitted			145.30	23.30	1.50
Retrofitted with SC-PC enlarged beams		(NLTH)	98.70	0.00	1.10
		Proposed	87.00	0.00	0.84
3D					
Un-retrofitted			95.00	33.20	1.20
Retrofitted with SC-PC enlarged beams	Three	(NLTH)	88.00	1.80	1.10
		Proposed	108.00	0.00	1.15
	Six	(NLTH)	70.10	0.80	0.80
		Proposed	96.00	0.00	1.02
	Nine	(NLTH)	60.00	2.80	0.72
		Proposed	84.00	0.00	0.92
Retrofitted with SC-PC prismatic beams	Three	(NLTH)	96.70	0.60	1.20
		Proposed	102.00	0.00	1.24
	Six	(NLTH)	84.70	1.50	1.00
		Proposed	93.30	0.00	1.10
	Nine	(NLTH)	62.70	1.30	0.70
		Proposed	84.00	0.00	1.00

Offprint provided courtesy of www.icevirtuallibrary.com
Author copy for personal use, not for distribution

1.1%. In addition, the results of the proposed method are found to be in good agreement with the mean responses obtained from the NLTH analysis. The percentage difference between the static and the dynamic analyses is around 12% in the case of maximum roof displacement and approximately 30% in the case of MIDR. The results are almost identical in the case of residual drift.

For comparison purposes, three-bay and six-bay SC-PC frames are applied for retrofit and the seismic performances are investigated. Figure 13 shows the MIDR of the 3D model structure retrofitted with three-bay, six-bay and nine-bay SC-PC frames subjected to the selected earthquake ground motions. It can be observed that retrofitting the structure with nine-bay SC-PC frames is much more effective than in the case of three-bay or six-bay SC-PC frames in reducing the MIDR. Retrofit with a nine-bay SC-PC frame results in MIDR value less than or equal to 0.8%, which is suitable for satisfying the life safety limit state. Owing to the plan asymmetry along the x (long) direction of the 3D model structure, the centre of mass does not coincide with the centre of stiffness. It is observed in the analysis results that the maximum drift ratio between the two corner points is 1.08, which is less than the criterion to be considered as a structure with torsional irregularity according to ASCE 7-16.

Table 4 summarises the maximum roof displacement, the residual drift and the MIDR results of the 3D frame using the static (proposed method) and dynamic analyses. SC-PC frames with three different numbers of bays are investigated using the proposed beam-end shape. The same table summarises the same analysis results obtained using the prismatic beams. The table shows that, in the case of maximum roof displacement, the retrofitted 3D model provides an upper bound for the three cases (three-bay, six-bay and nine-bay SC-PC frame). The un-retrofitted model has an average maximum roof displacement of 95.0 mm from the earthquake records set; however, this value is reduced to 88.0, 70.1 and 60.0 mm, respectively, in the retrofitted structure with three-bay, six-bay and nine-bay SC-PC frame. For the case of the SC-PC frame retrofit using conventional beams, as shown in the table, these values are 96.7, 84.7 and 62.7 mm, respectively. This means that the retrofit scheme using conventional prismatic PC beams provides an upper bound for the maximum roof displacement for the retrofit with the proposed beam shapes.

The residual drift, shown in Table 4, is reduced from 33.2 mm for the un-retrofitted model to almost zero for the retrofitted model. This is true for both the retrofit with conventional and proposed beams. The average MIDR for the un-retrofitted model is 1.2%, which is reduced to 1.1, 0.8 and 0.7% in the structure retrofitted with three-bay, six-bay and nine-bay SC-PC frames, respectively, having the proposed beam shape. However, these values are increased to 1.2, 1.0 and 0.72%, respectively, in the retrofitted structure with conventional

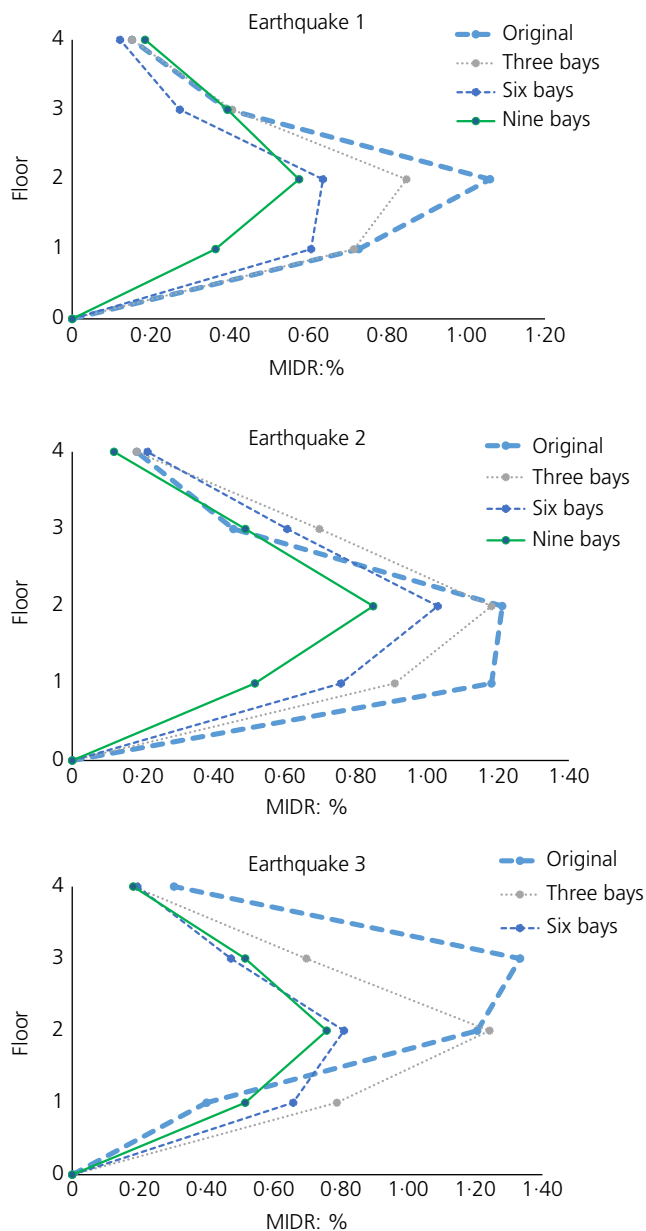


Figure 13. MIDR of the 3D model structure retrofitted with SC-PC frames having the proposed beam-end shape

prismatic beams. This indicates that, compared with the MIDR of the structure retrofitted with conventional beams, the MIDR of the structure retrofitted with enlarged beam ends is reduced by 9.0, 25.0 and 2.8%, respectively, in the structure with three-bay, six-bay and nine-bay SC-PC frames. It can be observed that the relative effectiveness of the proposed enlarged beam-end shape is more pronounced when the overall stiffness (i.e. the number of bays) of the SC-PC frame is small. Figure 14 shows the average values of the three earthquakes for maximum displacement, residual displacement and MIDR of the 3D model structure before and after retrofit.

Offprint provided courtesy of www.icevirtuallibrary.com
Author copy for personal use, not for distribution

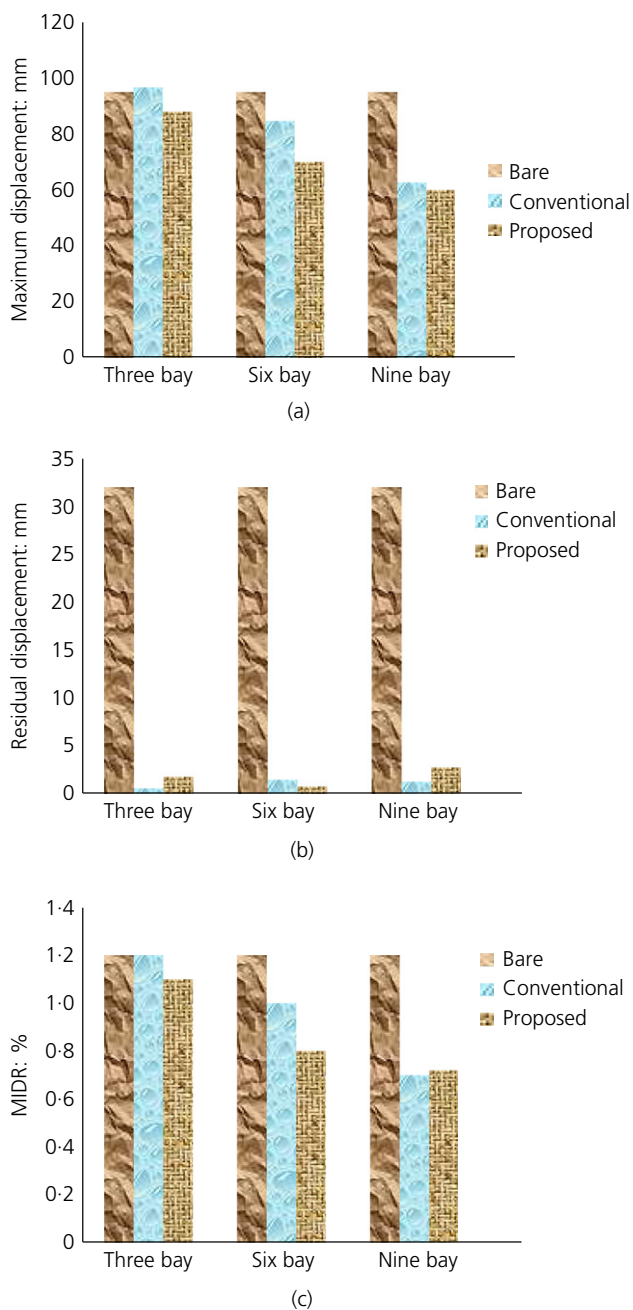


Figure 14. The average values of the three earthquakes for (a) maximum displacement, (b) residual displacement and (c) MIDR of the 3D model structure before and after retrofitting

Conclusions

The main findings of the current study are summarised as follows.

- The SC-PC frames turned out to be effective in reducing seismic response of the 2D and 3D low-rise RC structures, which are not designed for seismic loads, by providing both additional stiffness and self-centring force.

- The proposed design procedure, which is based on the initial stiffness of the un-retrofitted structure and stiffness graphs of the SC-PC frames, turned out to be simple and convenient to predict the initial stiffness of the required SC-PC frames for retrofitting.
- The proposed procedure was especially effective in providing a retrofit scheme that eliminates the residual drift of both the 2D and 3D case study structures.
- For the 2D case, the maximum roof displacement was reduced from 145.3 to 98.7 mm, the residual drift was reduced from 23.3 mm to zero, and the MIDR was reduced from 1.5 to 1.1%. The results of the proposed method were found to be in good agreement with the mean responses obtained from the NLTH analysis, especially for the residual drift.
- For the 3D case, the nine-bay SC-PC frames were found to be more effective than the three-bay and six-bay frames for reducing the MIDR. The average MIDR from the NLTH analysis for the selected earthquake records showed that the nine-bay SC-PC can limit the MIDR below 0.8%. This is a preferable immediate occupancy limit state for important structures such as schools, where stringent limit states are usually applied.
- The enlarged SC-PC beam-end shape proposed in this study contributed to enhancing the re-centring moment capacity of the SC-PC frames more effectively compared with the conventional prismatic beams.
- The non-linear dynamic time history analysis results indicated that, compared with the MIDR of the structure retrofitted with conventional beams, the MIDR of the structure retrofitted with enlarged beam ends was further reduced by 9.0, 25.0 and 2.8%, respectively, in the structure with three-bay, six-bay and nine-bay SC-PC frames.
- In this study, the SC-PC frame was applied to seismic retrofit of structures having small to medium natural period with insignificant higher mode effect for applying the equal displacement rule. Further research is needed for the seismic retrofit of structures with significant participation of higher modes.

Acknowledgement

This research was supported by Basic Science Research Program through the National Research Foundation of Korea (NRF-2019R1F1A1B01060877).

REFERENCES

- ACI (American Concrete Institute) (2014) ACI 318R-14: Building code requirements for structural concrete (ACI 318-14) and commentary. ACI, Farmington Hills, MI, USA.
- ASCE (American Society of Civil Engineers) (2013) ASCE/SEI 41-13: Seismic evaluation and retrofit of existing buildings. ASCE, Reston, VA, USA.
- ASCE (2016) ASCE/SEI 7: Minimum design loads for buildings and other structures. ASCE, Reston, VA, USA.

Offprint provided courtesy of www.icevirtuallibrary.com
Author copy for personal use, not for distribution

- Bedoya-Ruiz D, Bermúde CA, Álvarez DA and Ortiz GA (2012) Cyclic behavior of prestressed precast concrete walls. *Proceedings of 15th World Congress on Earthquake Engineering, Lisbon, Portugal*. Sociedade Portuguesa de Engenharia Sismica, Lisbon, Portugal, vol. 25, pp. 19578–19585.
- Belleri A, Marini A, Paolo R and Nascimbene R (2017) Dissipating and re-centering devices for portal-frame precast structures. *Engineering Structures* **150**: 736–745.
- Binici B and Mosalam KM (2007) Analysis of reinforced concrete columns retrofitted with fiber reinforced polymer lamina. *Composites: Part B* **38(2)**: 265–276.
- Buchanan AH, Bull D, Dhakal R et al. (2011) *Base Isolation and Damage-Resistant Technologies for Improved Seismic Performance of Buildings*. University of Canterbury, Christchurch, New Zealand, Technical Report 2011-02 for the Royal Commission of Inquiry into building failure caused by the Canterbury earthquakes.
- Cao Z, Guo T, Xu Z and Lu S (2015) Theoretical analysis of self-centering concrete piers with external dissipators. *Earthquakes and Structures, An International Journal* **9(6)**: 1313–1336.
- Celik O and Sritharan S (2004) *An Evaluation of Seismic Design Guidelines Proposed for Precast Concrete Hybrid Frame Systems*. Iowa State University of Science and Technology, Ames, IA, USA, ISU-ERI-Ames Report ERI-04425, submitted to the Precast/Prestressed Concrete Manufacturers Association of California, Final report.
- CEN (European Committee for Standardization) (2004) Eurocode 8: Design of structures for earthquake resistance – Part 1: General rules, seismic actions rules for buildings. CEN, Brussels, Belgium.
- Chancellor NB, Eatherton MR, Roke DA and Akbaş T (2014) Self-centering seismic lateral force resisting systems: high performance structures for the city of tomorrow. *Buildings* **4(3)**: 520–548.
- CSI (Computers and Structures, Inc) (2015) *SAP2000, Ver. 18: Analysis Reference Manual*. Computer and Structures, Inc, Berkeley, CA, USA.
- Dezfuli MA, Dolatshahi KM, Mofid M and Eshkevari SS (2017) Coreless self-centering braces as retrofit devices in steel structures. *Journal of Constructional Steel Research* **133**: 485–498.
- Dyanati M, Huang Q and Roke D (2017) Cost–benefit evaluation of self-centering concentrically braced frames considering uncertainties. *Journal of Structure and Infrastructure Engineering* **13(5)**: 537–553.
- Eatherton MR, Ma X, Krawinkler H, Deierlein GG and Hajjar JF (2014) Quasi-static cyclic behavior of controlled rocking steel frames. *Journal of Structural Engineering* **140(11)**, [https://doi.org/10.1061/\(ASCE\)ST.1943-541X.0001005](https://doi.org/10.1061/(ASCE)ST.1943-541X.0001005).
- Englekirk RE (2002) Design–construction of the Paramount – a 39-story precast prestressed concrete apartment building. *PCI Journal* **47(4)**: 56–71.
- Fajfar P (2000) A nonlinear analysis method for performance-based seismic design. *Earthquake Engineering and Structural Dynamics* **16(3)**: 573–592.
- Fajfar P (2002) Structural analysis in earthquake engineering – a breakthrough of simplified non-linear methods. *Proceedings of 12th European Conference on Earthquake Engineering, London, UK*. Elsevier, Amsterdam, the Netherlands, paper no. 843, pp. 1–20.
- Guo T, Xu Z, Song L, Wang L and Zang Z (2017) Seismic resilience upgrade of RC frame building using self-centering concrete walls with distributed friction devices. *Journal of Structural Engineering* **143(12)**, <https://doi.org/10.1061/%28ASCE%29ST.1943-541X.0001901>.
- Henry RS, Sritharan S and Ingham JM (2016) Residual drift analyses of realistic self-centering concrete wall systems. *Earthquakes and Structures* **10(2)**: 409–428.
- Holden T, Restrepo J and Mander JB (2003) Seismic performance of precast reinforced and prestressed concrete walls. *Journal of Structural Engineering* **129(3)**: 286–296.
- Hu X and Zhang Y (2013) Ductility demand of partially self-centering structures under seismic loading: SDOF systems. *Earthquakes and Structures* **4(4)**: 365–381.
- Hu X, Zhang Y and Nasim S. Moghaddasi B (2012) Seismic performance of reinforced concrete frames retrofitted with self-centering hybrid wall. *Advances in Structural Engineering* **15(12)**: 2131–2144.
- Kim J and Seo Y (2003) Seismic design of steel structures with buckling-restrained knee braces. *Journal of Constructional Steel Research* **59(12)**: 1477–1497.
- Kurama YC, Weldon BD and Shen Q (2006) Experimental evaluation of post-tensioned hybrid coupled wall sub-assemblages. *Journal of Structural Engineering* **132(7)**: 1017–1029.
- Mattcock AH (1979) Flexural strength of prestressed concrete sections by programmable calculator. *PCI Journal* **24(1)**: 26–37.
- Naeem A and Kim J (2018) Seismic retrofit of a framed structure using damped cable system. *Steel and Composite Structures* **29(3)**: 287–299.
- Nikbakht E, Rashid K, Hejazi F and Osman SA (2015) Application of shape memory alloy bars in self-centering precast segmental columns as seismic resistance. *Structure and Infrastructure Engineering* **11(3)**: 297–309.
- NourEldin M, Naeem A and Kim J (2019) Life-cycle cost evaluation of steel structures retrofitted with steel slit damper and shape memory alloy-based hybrid damper. *Advances in Structural Engineering* **22(1)**: 3–16.
- Park J, Lee J and Kim J (2012) Cyclic test of buckling restrained braces composed of square steel rods and steel tube. *Steel and Composite Structures* **13(5)**: 423–436.
- PEER (Pacific Earthquake Engineering Research) Center (2017) *Strong Motion Database*. PEER, Berkeley, CA, USA. See <https://peer.berkeley.edu/peer-strong-ground-motion-databases>.
- Priestley MN (1991) Overview of PRESSS research program. *PCI Journal* **36(4)**: 50–57.
- Priestley MN (1996) The PRESSS program: current status and proposed plans for phase III. *PCI Journal* **41**: 22–40.
- Priestley NMJ, Sritharan S, Conley JR and Pampanin S (1999) Preliminary results and conclusions from the PRESSS five-story precast concrete test building. *PCI Journal* **44**: 42–67.
- Rahman MA and Sritharan S (2007) Performance-based seismic evaluation of two five-story precast concrete hybrid frame buildings. *Journal of Structural Engineering* **133(11)**, [https://doi.org/10.1061/\(ASCE\)0733-9445\(2007\)133:11\(1489\)](https://doi.org/10.1061/(ASCE)0733-9445(2007)133:11(1489)).
- Roke DA (2010) *Damage-Free Seismic-Resistant Self-Centering Concentrically-Braced Frames*. PhD thesis, Lehigh University, Bethlehem, PA, USA.
- Song LL and Guo T (2017) Probabilistic seismic performance assessment of self-centering prestressed concrete frames with web friction devices. *Earthquakes and Structures, An International Journal* **12(1)**: 109–118.
- Takeuchi T, Chen X and Mats R (2015) Seismic performance of controlled spine frames with energy-dissipating members. *Journal of Constructional Steel Research* **114**: 51–65.

How can you contribute?

To discuss this paper, please submit up to 500 words to the editor at journals@ice.org.uk. Your contribution will be forwarded to the author(s) for a reply and, if considered appropriate by the editorial board, it will be published as a discussion in a future issue of the journal.